

**High flux high-silica SSZ-13 membrane for CO<sub>2</sub> separation**

Journal:	<i>Journal of Materials Chemistry A</i>
Manuscript ID:	TA-ART-05-2014-002744.R1
Article Type:	Paper
Date Submitted by the Author:	18-Jun-2014
Complete List of Authors:	Kosinov, Nikolay; Eindhoven University of Technology, Department of Chemical Engineering and Chemistry Auffret, Clement; Eindhoven University of Technology, Department of Chemical Engineering and Chemistry Gücüyener, Canan; Delft University of Technology, Chemical Engineering Szyja, Bartłomiej; University of Münster, Institute for Solid State Theory Gascon, Jorge; Delft University of Technology, Chemical Engineering; TUDelft, Chemical Engineering Kapteijn, Freek; TUDelft, Chemical Engineering Hensen, Emiel; Eindhoven University of Technology, Department of Chemical Engineering and Chemistry

## ARTICLE

## High flux high-silica SSZ-13 membrane for CO<sub>2</sub> separation

Cite this: DOI: 10.1039/x0xx00000x

Nikolay Kosinov<sup>a</sup>, Clement Auffret<sup>a</sup>, Canan Gücüyener<sup>b</sup>, Bartłomiej M. Szyja<sup>c</sup>, Jorge Gascon<sup>b</sup>, Freek Kapteijn<sup>b</sup> and Emiel J.M. Hensen<sup>a\*</sup>Received 00th January 2014,  
Accepted 00th January 2014

DOI: 10.1039/x0xx00000x

www.rsc.org/

High-silica (gel Si/Al = 100) SSZ-13 membranes were prepared by hydrothermal secondary growth on the surface of  $\alpha$ -alumina hollow fiber supports. The membranes were evaluated for their performance in the separation of CO<sub>2</sub> from equimolar mixtures with CH<sub>4</sub> or N<sub>2</sub>. The maximum CO<sub>2</sub>/CH<sub>4</sub> and CO<sub>2</sub>/N<sub>2</sub> separation selectivities were found to be 42 and 12 respectively, with a high CO<sub>2</sub> permeance of  $3.0 \times 10^{-7}$  mol.m<sup>2</sup>.s<sup>-1</sup>.Pa<sup>-1</sup> at 293 K and total feed pressure of 0.6 MPa. At the low aluminum content, the prepared membranes contain a very low number of defects, as follows from their H<sub>2</sub>/SF<sub>6</sub> ideal selectivity of over 500 in the 293-473 K temperature range. Due to their hydrophobicity, water in the feed mixture has only a small influence on the permeance at temperatures above 353 K. Water improves the CO<sub>2</sub>/N<sub>2</sub> and CO<sub>2</sub>/CH<sub>4</sub> selectivity, which is attributed to preferential blocking of the hydrophilic, non-zeolitic defect pores. The hydrothermal stability of high-silica SSZ-13 membrane was evaluated by a long (220 h) CO<sub>2</sub>/N<sub>2</sub> separation test with a humidified (9.5 kPa H<sub>2</sub>O) feed mixture at 393 K and 0.6 MPa feed pressure. The permeance and selectivity were stable during this endurance test, underpinning the promise of high-silica SSZ-13 membranes for application in the separation of hot and humid gas mixtures.

### Introduction

Carbon dioxide emissions are a source of major global environmental concern, as consensus is growing about its involvement in global warming.<sup>1</sup> Carbon capture and sequestration and utilization (CCS and CCU)<sup>2,3</sup> are considered promising strategies to limit anthropogenic CO<sub>2</sub> emissions.<sup>4</sup> Capturing CO<sub>2</sub> is technologically very challenging and it is estimated to account for 50-90 % of the total cost in the CCS/CCU chain.<sup>5</sup> The benchmark technology for CO<sub>2</sub> capture is chemical absorption using amines.<sup>6,7</sup> Drawbacks of this industrial process are the cyclic operation and the high energy penalty.<sup>8</sup> Typically, values over 2.5 GJ/tonne of CO<sub>2</sub> are used to liberate CO<sub>2</sub> from its adduct with amines.<sup>9</sup> Thus, there is a clear need for energy-efficient processes to capture CO<sub>2</sub> from flue and natural gas sources.

Membrane technology constitutes one of the most promising and energy-efficient separation methods.<sup>10</sup> For CO<sub>2</sub> separation from gas mixtures, various membranes have been explored such as organic,<sup>11</sup> inorganic,<sup>12</sup> MOF,<sup>13</sup> and mixed-matrix membranes.<sup>14,15</sup> Zeolites (crystalline porous aluminosilicates) are especially interesting for membrane preparation due to their uniform system of pores with molecule-sized dimensions, high porosity and excellent thermal and chemical stability.<sup>16,17,18</sup> Accordingly, zeolite membranes can offer high diffusion selectivity to small and moderate adsorption selectivity to strongly adsorbing molecules.<sup>19</sup> There is a great variety in the pore structure of zeolites, allowing

selection of suitable pore diameter and shape for targeted separations. Besides size, also the pore system dimensionality and the polarity of zeolites influence the performance and the application window of zeolite membranes/films. For instance, MFI, which is the most investigated zeolite for membrane preparation,<sup>20,21,22</sup> has a three-dimensional system of channels with a size of ca. 0.55 nm enclosed by rings of 10 oxygen atoms. Typically, such 10-membered, and also 12-membered pore systems (pore openings ~0.74 nm), offer only adsorption selectivity for separation of permanent gases.<sup>23</sup> Accordingly, there is also substantial interest in the development of membranes using zeolites with smaller pores.<sup>24</sup> As such, 8-membered ring (8MR) zeolites are promising for gas separation, because their pores in the range of 0.3-0.4 nm are comparable to the kinetic diameters of permanent gases (e.g., 0.28 nm for H<sub>2</sub>, 0.33 nm for CO<sub>2</sub>, 0.36 nm for N<sub>2</sub> and 0.38 nm for CH<sub>4</sub>). If the size of a molecule is close to the pore size, configurational diffusion effects arise resulting in high gas separation selectivity.

To date the number of attempts to prepare zeolite membranes in the form of thin polycrystalline films for application in CO<sub>2</sub> separation is limited. Table 1 summarizes the main achievements in this field. SAPO-34, a silicoaluminophosphate with the chabazite topology containing 8-membered rings, has shown promise for CO<sub>2</sub>/CH<sub>4</sub> and CO<sub>2</sub>/N<sub>2</sub> separation.<sup>25,26</sup> SAPO-34 membranes display high permeance and selectivity, even at pressures as high as 10 MPa as a result of the combination of adsorption selectivity and

molecular sieving effects.<sup>27</sup> An important drawback of silicoaluminophosphates is their hydrophilicity and, related to this, low stability under humid conditions.<sup>28</sup> Thus, the separation performance of SAPO-34 membranes is greatly disturbed by the presence of water.<sup>29</sup> Low-silica aluminosilicate membranes are also highly hydrophilic and usually exhibit a large number of defects in the film, opening non-zeolitic pathways for unselective mass transport, as discussed by Caro and co-workers.<sup>30,31</sup> The use of high-silica hydrophobic DDR membranes, first prepared by Tomita *et al.*,<sup>32</sup> is more promising as these are stable under humid conditions.<sup>33</sup> A drawback of the two-dimensional pore system of DDR is the relatively low permeance through the membrane and the challenge to reproducibly synthesize such membranes. Compared to DDR, SSZ-13, which is the aluminosilicate analogue of SAPO-34, has the advantage of a three-dimensional pore system with 0.38 nm openings and a much lower framework density (higher

porosity). It can also be synthesized in high-silica form.<sup>34</sup> It was recently reported that SSZ-13 is a selective sorbent for CO<sub>2</sub>,<sup>35,36</sup> whose performance is not disturbed by the presence of water.<sup>37</sup> So far, only low-silica SSZ-13 membranes have been synthesized, with Si/Al ratios below 20.<sup>38,39,40,41</sup> Although these rather hydrophilic membranes display good performance in dewatering of organic/water mixtures, their selectivity in gas separation is usually too low due to the large number of defects.<sup>42</sup>

Here, we report for the first time a reproducible synthesis of high-silica SSZ-13 (Si/Al ratio higher than 80) membranes. These membranes show very good performance in the separation of CO<sub>2</sub>/N<sub>2</sub> and CO<sub>2</sub>/CH<sub>4</sub> mixtures. We show that the presence of water decreases the permeance but improves CO<sub>2</sub> selectivity. Excellent stability of high-silica SSZ-13 membranes under humid conditions at elevated temperature is validated by a long-term endurance test.

**Table 1** Typical performance of supported zeolite membranes in CO<sub>2</sub> separation

Membrane/support	Pores, nm	Separation	Temperature, K	Feed pressure, MPa	CO <sub>2</sub> Permeance, 10 <sup>-7</sup> mol. m <sup>-2</sup> .s <sup>-1</sup> .Pa <sup>-1</sup>	Selectivity	Remark
Na-Y/ $\alpha$ -alumina <sup>43</sup>	0.74	CO <sub>2</sub> /H <sub>2</sub>	298	0.1	7	28	Wicke-Kallenbach (WK) method Si/Al = 1.5
		CO <sub>2</sub> /N <sub>2</sub>	298	0.1	10	40	
Na-X/ $\alpha$ -alumina <sup>44</sup>	0.74	CO <sub>2</sub> /N <sub>2</sub>	296	0.1	0.5	8	Si/Al < 1.5, WK
Silicalite-1/SS <sup>24</sup>	0.55	CO <sub>2</sub> /CH <sub>4</sub>	200	0.1	0.75	20	Pure-silica, WK
Silicalite-1/ $\alpha$ -alumina <sup>45</sup>	0.55	CO <sub>2</sub> /H <sub>2</sub>	238	0.9	51	109	Pure-silica uniformly oriented film
ZSM-5/ $\alpha$ -alumina <sup>46</sup>	0.55	CO <sub>2</sub> /CH <sub>4</sub>	295	1	45	6	Si/Al > 100, membrane thickness ca. 700 nm
		CO <sub>2</sub> /H <sub>2</sub>	296	1	93	22	
LTA/ $\alpha$ -alumina <sup>47</sup>	0.41	H <sub>2</sub> /CO <sub>2</sub>	373	0.1	0.12	12.5	Si/Al = 1, WK Multilayer LTA membrane prepared with addition of APTES
SSZ-13/SS <sup>40</sup>	0.38	CO <sub>2</sub> /CH <sub>4</sub>	298	0.22	1.7	13	Si/Al = 13.3
		CO <sub>2</sub> /N <sub>2</sub>	298	0.22	1.9	11	
SAPO-34/SS <sup>48</sup>	0.38	CO <sub>2</sub> /CH <sub>4</sub>	295	3	1.0	60	Silicoaluminophosphate
SAPO-34/ $\alpha$ -alumina <sup>49</sup>	0.38	CO <sub>2</sub> /CH <sub>4</sub>	295	4.6	16	70	Silicoaluminophosphate
SAPO-34/SS <sup>50</sup>	0.38	CO <sub>2</sub> /CH <sub>4</sub>	295	0.1	25	9	Silicoaluminophosphate WK
DDR/ $\alpha$ -alumina <sup>51</sup>	0.36	CO <sub>2</sub> /CH <sub>4</sub>	298	0.1	0.12	98	Siliceous, WK
		CO <sub>2</sub> /air	303	0.1	0.6	30	
DDR/ $\alpha$ -alumina <sup>52</sup>	0.36	CO <sub>2</sub> /CH <sub>4</sub>	303	0.1	0.55	1000	Siliceous, WK
		CO <sub>2</sub> /N <sub>2</sub>	308	0.1	0.39	104	
Zeolite T/mullite <sup>53</sup>	0.36; 0.66	CO <sub>2</sub> /N <sub>2</sub>	308	0.1	0.39	104	Si/Al = 3-4 Vacuum on the permeate side
		CO <sub>2</sub> /CH <sub>4</sub>	308	0.1	0.46	400	

## Experimental

### Materials

Symmetric hollow fiber  $\alpha$ -alumina supports (i.d. 1.8 mm, o.d. 2.9 mm, total length of 70 mm and permeation area of 1.7 cm<sup>2</sup>) with pores of ca. 300 nm and a porosity of ca. 30 %, were

supplied by Hyflux. Prior to deposition of the zeolite layer the supports were boiled in a mixture of 1 HCl : 1 H<sub>2</sub>O<sub>2</sub> : 6 H<sub>2</sub>O for 30 min at 373 K followed by rinsing in distilled water to remove possible impurities. After cleaning both ends of each support were sealed with ceramic glaze (Kera Dekor 5602, UHLIG, Germany) and the fibers were finally fired at 1300 K. Fumed silica (Cab-O-Sil® M-5, Cabot), N,N,N-trimethyl-1-adamant

ammonium hydroxide (TMAdaOH 25%, SACHEM, Inc.), sodium hydroxide NaOH (50%, Merck), aluminum hydroxide Al(OH)<sub>3</sub> (Sigma-Aldrich) and demineralized water were used for preparation of SSZ-13 films.

### Membrane synthesis

Supported membranes were prepared by seeded secondary growth. Firstly, SSZ-13 seed crystals were prepared by mixing NaOH and TMAdaOH with water in a PTFE beaker, followed by addition of Al(OH)<sub>3</sub>. The mixture was thoroughly stirred until all the Al(OH)<sub>3</sub> was completely dissolved (ca. 30 min). Fumed silica was then added and the gel was aged for 6 h under continuous stirring at room temperature. The initial gel composition was 20 TMAdaOH: 20 NaOH: 1.3 Al(OH)<sub>3</sub>: 104 SiO<sub>2</sub>: 4400 H<sub>2</sub>O. After ageing, the mixture was poured in a stainless steel autoclave (120 mL) equipped with a PTFE liner. After closing, the autoclave was placed in a preheated oven and hydrothermal synthesis was statically performed at 433 K for 144 h. The SSZ-13 crystals were recovered by filtration and then thoroughly washed. The as-synthesized crystals were too large (ca. 10 μm) to directly use them as seeds. Thus, wet ball milling was performed in accordance with the procedure described by Charkhi *et al.*<sup>54</sup> To achieve a narrow seed size distribution (ca. 120 nm), the obtained mixture is diluted and centrifuged. The final solid content of the seed solution was ca. 0.5%. The inner surface of the α-alumina support was coated with a layer of SSZ-13 nano-crystals by dip-coating. For this purpose, the supports were brought into contact with the suspension for 10-15 s. After coating, the seeded supports were dried at 383 K overnight. The complete seeding procedure was repeated twice to obtain a dense and uniform seed layer (Fig. S1).

The synthesis gel for secondary growth was prepared in the same way as the synthesis gel for the seed crystals, with the only difference of slightly higher Si/Al ratio (100). The initial gel composition was 20 TMAdaOH: 20 NaOH: 1.05 Al(OH)<sub>3</sub>: 105 SiO<sub>2</sub>: 4400 H<sub>2</sub>O. The aged gel was poured in a PTFE-lined autoclave (45 mL) in which the pre-seeded fiber supports, wrapped with PTFE tape, were vertically placed. Secondary growth was carried out in static conditions at 433 K for 144 h. After synthesis the membranes were washed by copious amounts of demineralised water and dried at 383 K overnight. For XRD analysis SSZ-13 films were also prepared on porous α-alumina disc supports (Pervatech) by the same procedure.

The organic template was removed from the SSZ-13 pores by an optimized calcination program in pure oxygen flow at 723 K for 80 h with heating and cooling rates of 0.2 K/min. This method was applied because a conventional detemplation program (823 K, air) yielded cracks in the membrane layer (see Figs. S3-S4).

### Adsorption isotherms

Gas adsorption measurements on SSZ-13 zeolite powders were performed using a Tristar II 3020 Micromeritics sorptometer employing high-purity CO<sub>2</sub>, CH<sub>4</sub> and N<sub>2</sub> gases (99.99 %). The zeolite powder was calcined at 650 °C with a heating rate of 0.5 °C/min for 7 h. Prior to the measurements, the adsorbent was outgassed at 250 °C under vacuum for 16 h. Details of the baths used for attaining different temperatures for the adsorption measurements are given in Supporting Information.

### Molecular simulations

Adsorption isotherms were computed using a force field based approach. The force field was taken from García-Pérez *et al.*<sup>55</sup> The force field consists of electrostatic and dispersive terms described by the Coulomb and Lennard-Jones models, respectively. The static charges are 2.05 for Si atoms and -1.025 for O atoms. Long-range electrostatic interactions in the periodic simulation cell were taken into account using the Ewald summation. Van der Waals forces were described by the effective potential acting on the oxygen atoms, and silicon atoms were excluded. All zeolite atoms were held rigid during the simulations. Methane is represented by the united atom model with no charge assigned. N<sub>2</sub> is represented by the rigid dumbbell model with an interatomic distance of 1.098 Å. The partial charges of the N atoms are -0.40484, which are compensated by a dummy charge of +0.80968 placed at the molecule center. CO<sub>2</sub> has rigid bond lengths of 1.16 Å, and charges of +0.6512 and -0.3256 on C and O atoms, respectively. The Lennard-Jones potential is truncated at a distance of 12 Å. The simulations were carried out using Materials Studio 6.0 (Accelrys). The Metropolis method was employed. The number of steps was set to 20 million to ensure proper equilibrium. Adsorption isotherms were determined for N<sub>2</sub>, CO<sub>2</sub>, CH<sub>4</sub> and for CO<sub>2</sub>/N<sub>2</sub>, CO<sub>2</sub>/CH<sub>4</sub> equimolar mixtures in the pressure range from 10 kPa to 1000 kPa at a temperature of 293 K. The CHA model was taken from the Materials Studio library of structures. The unit cell was multiplied three times in each direction to exceed the minimum of 20 Å size to maintain the consistency with the force field. In total the simulation system contained 324 Si and 648 O atoms. In these simulations the presence of framework Al atoms and, consequently, also that of Na atoms was neglected because of their low abundance.

### Membrane characterization

Supported SSZ-13 films were characterized by X-ray diffraction (XRD), scanning electron microscopy (SEM) and X-ray photoelectron spectroscopy (XPS). The separation performance was evaluated by single gas permeation (H<sub>2</sub>, CO<sub>2</sub>, CH<sub>4</sub>, N<sub>2</sub> and SF<sub>6</sub>) as well as separation measurements of equimolar CO<sub>2</sub>/CH<sub>4</sub> and CO<sub>2</sub>/N<sub>2</sub> mixtures.

The structure of the zeolite film was determined by recording XRD patterns with a Bruker D4 Endeavour Diffractometer using Cu Kα-radiation in the 2θ range of 5-50° on the disc support. The chemical composition of the SSZ-13 films was analysed by a Thermo Scientific K-alpha XPS spectrometer equipped with a monochromatic Al Kα X-ray source.

An in-house built setup (Fig. S2) was used for permeation measurements (pressure and temperature ranges of 0.1-0.6 MPa and 293-473 K, respectively). Helium was used as the sweep gas for all the measurements, except when H<sub>2</sub> was one of the permeating gases in which case Ar was employed as the sweep gas. The CO<sub>2</sub>/CH<sub>4</sub> and CO<sub>2</sub>/N<sub>2</sub> separation tests were also performed in the pressure gradient mode at a feed pressure of 0.6 MPa (Figs. S5-S6). The permeate side was kept at atmospheric pressure. The composition of the feed, permeate and retentate gas was measured by an online gas chromatograph (Interscience Compact GC) equipped with two Rtx-1.5u columns, a Molsieve 5A column, a flame-ionization detector (FID) and two thermal conductivity detectors (TCD). Gas flows were measured by digital and soap film flow meters. The selectivity was calculated as the ratio of permeances of two components. To determine the influence of moisture on the membrane performance the feed gas mixture was humidified by

using a stainless steel saturator, containing demineralised water, kept in thermostat to control water vapour pressure.

## Results and Discussion

### Membrane synthesis

As-synthesized SSZ-13 films contain TMAda template molecules blocking the zeolite pores. Accordingly, before detemplation high-quality membranes should be impermeable to any gas. To determine the quality of the as-synthesized membranes, the CH<sub>4</sub> permeance at 293 K and 0.6 MPa was determined. All the as-synthesized membranes displayed low CH<sub>4</sub> permeance in the order of  $1\text{--}3 \times 10^{-10} \text{ mol.m}^{-2}.\text{s}^{-1}.\text{Pa}^{-1}$ . Such low values are indicative of the very small number of macro-defects in the as-synthesized membranes. After calcination the membranes were analysed by SEM (Fig. 1), which revealed that rather thin and uniform polycrystalline films with a thickness of 4–6  $\mu\text{m}$  were formed on the alumina support surface. No microscopic defects were observed, except for the presence of some larger single crystals nucleated from the bulk. Furthermore, the images show that the boundary between the zeolite layer and the support was well defined. Clearly, the support layer has not been infiltrated by the growing zeolite. Although infiltration may improve the adherence between the zeolite layer and the support, it would negatively affect the overall permeability. The XRD pattern of the SSZ-13 film confirms the purity of the CHA crystalline phase. There is no specific orientation of the crystals, so that the layer can be considered to be randomly oriented. The Si/Al ratio of the film as measured by XPS is 86, which is slightly lower than the Si/Al ratio of 100 in the synthesis mixture. The lower Si/Al ratio is likely due to leaching of some Al from the  $\alpha$ -alumina support as previously discussed.<sup>56,57</sup>

### Reproducibility of membrane synthesis

Reproducible production of zeolite membranes by hydrothermal synthesis is not an easy task.<sup>58,59</sup> To investigate the reproducibility of the SSZ-13 membrane synthesis six independently prepared and calcined membranes were tested in the separation of equimolar mixtures of CO<sub>2</sub>/N<sub>2</sub> and CO<sub>2</sub>/CH<sub>4</sub> as well as single gas permeation of SF<sub>6</sub>. The SF<sub>6</sub> molecule having a kinetic diameter of 0.55 nm can only permeate through defects and, accordingly, this test is a good measure of membrane quality.<sup>60</sup> Table 2 reports the separation and permeation data. The results show that the six membranes display similar performance, evidencing that our method yields high-quality membranes in a reproducible manner. We assign the minor deviations in membrane performance in part to the heterogeneity of the ceramic support. The extrusion-derived symmetric hollow fiber supports containing a rather rough and non-uniform surface exhibited some variation in the order of 10% in pure N<sub>2</sub> permeance ( $6.9 \pm 0.6 \times 10^{-6} \text{ mol.m}^{-2}.\text{s}^{-1}.\text{Pa}^{-1}$ ; 20 supports tested at room temperature and pressure drop of 0.05 MPa). After reproducibility tests sample M-1 was chosen for further separation characterization.

**Table 2** Reproducibility of membrane preparation

Sample	Selectivity		Permeance, $10^{-7} \text{ mol.m}^{-2}.\text{s}^{-1}.\text{Pa}^{-1}$		
	CO <sub>2</sub> /N <sub>2</sub>	CO <sub>2</sub> /CH <sub>4</sub>	CO <sub>2</sub> (N <sub>2</sub> )	CO <sub>2</sub> (CH <sub>4</sub> )	SF <sub>6</sub> ( $\times 10^3$ )
M-1 <sup>a</sup>	10.4±0.6	36.5	3.0±0.2	3.0	4.2
M-2	10.1	41.8	2.0	1.9	5.0
M-3	11.6	37.5	3.4	3.3	5.8
M-4	10.2	34.5	2.2	2.2	6.4
M-5	10.3	37.8	2.1	1.8	5.3
M-6	8.4	28.6	2.5	2.5	8.3
Average	10±2	36±7	2.5±1	2.5±1	6±2

Conditions: equimolar mixtures, 293 K, 0.6 MPa feed pressure, atm. pressure on permeate side, total flow rate 200 ml/min, 200 ml/min of sweep gas He.

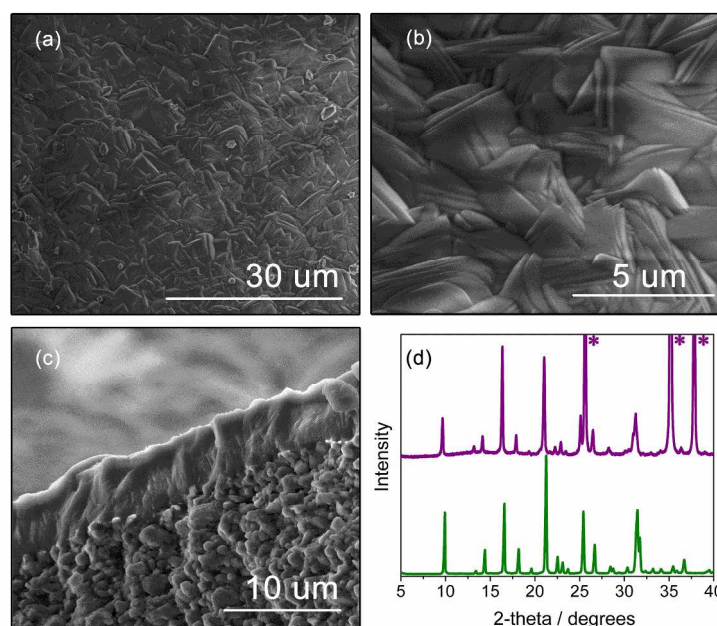


**Fig. 1** SEM (a,b) top view and (c) cross-section images of a SSZ-13 membrane prepared by secondary growth; (d) XRD patterns of CHA (SiO<sub>2</sub>) crystals prepared according to Eilertsen *et al.*<sup>61</sup> (bottom) and SSZ-13 film synthesized on the surface of porous  $\alpha$ -alumina disc (top). Reflections from  $\alpha$ -alumina are marked with asterisks.

### Single gas permeation

The results of single gas permeation measurements of gases differing in molecular size and adsorption strength are shown in Fig. 2. The SSZ-13 membrane displays a high permeance of H<sub>2</sub> and CO<sub>2</sub> for zeolite membranes, with values in the order of  $3 \times 10^{-7} \text{ mol.m}^{-2}.\text{s}^{-1}.\text{Pa}^{-1}$  at 293 K. We expect that the permeability and selectivity of these membranes can be further improved by using less resistant supports with higher porosity and by decreasing the zeolite layer thickness.<sup>62</sup>

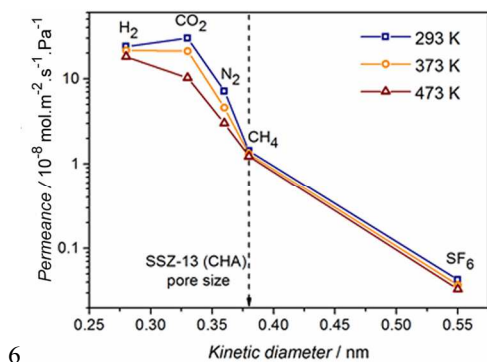


**Fig. 2** Dependence of single gas permeance on kinetic diameter (conditions: 0.6 MPa feed pressure, atmospheric pressure on permeate side, total flow rate 200 ml/min, 200 ml/min of sweep gas He).

The data in Table 3 clearly show that the membrane operates in the molecular sieving regime for SF<sub>6</sub>. The H<sub>2</sub>/SF<sub>6</sub> and H<sub>2</sub>/CH<sub>4</sub> ideal permselectivities are higher than 500 and 15, respectively, well above the respective values for the Knudsen selectivity of 8.5 and 2.8. As SF<sub>6</sub> is too large to permeate through the 8MR zeolite pores, the high H<sub>2</sub>/SF<sub>6</sub> ideal selectivity is also evidence for the low number of defects and high membrane quality. Diffusion of adsorbing gases through 8MR zeolites at moderate temperatures is governed by surface

diffusion. This phenomenon has been described in detail for DDR membranes by van den Bergh *et al.*<sup>63</sup> Briefly, with increasing temperature the concentration of adsorbed molecules becomes lower while the diffusivity increases. The net result is that depending on the respective temperature dependencies and conditions the permeation flux may increase, decrease or even pass through a maximum.<sup>64,65</sup> Here, the permeance of CO<sub>2</sub>, N<sub>2</sub>, CH<sub>4</sub> and H<sub>2</sub> decreases with increasing temperature (e.g. Figs. S5 and S6). SF<sub>6</sub> can only diffuse through defects in the zeolite film. Since permeation through pores much larger than 1 nm (Knudsen diffusion) scales inversely with the square root of the temperature, the SF<sub>6</sub> permeance decreases with increasing temperature. Moreover, the observation that the SF<sub>6</sub> permeance does not increase with temperature implies that neither additional defects are formed nor the existing defects become larger during heating of the membrane.

**Table 3** Ideal permselectivity at gas feed pressure of 0.6 MPa.

Temperature, K	293	373	473	Knudsen selectivity
CO <sub>2</sub> /CH <sub>4</sub>	20	16	8.3	0.6
CO <sub>2</sub> /N <sub>2</sub>	4.2	4.6	3.4	0.8
CO <sub>2</sub> /H <sub>2</sub>	1.3	1.0	0.6	0.2
H <sub>2</sub> /CH <sub>4</sub>	18	16	16	2.8
H <sub>2</sub> /SF <sub>6</sub>	560	580	550	8.5

### Gas mixture separation

Separation of equimolar mixtures of CO<sub>2</sub>/N<sub>2</sub> and CO<sub>2</sub>/CH<sub>4</sub> at varying pressure and composition was investigated next. Fig. 3 shows the influence of the total and partial pressures on the permeance and selectivity. At 293 K and 0.6 MPa feed pressure the mixture selectivity for both gas mixtures is 1.5-2 times higher than the ideal selectivity.

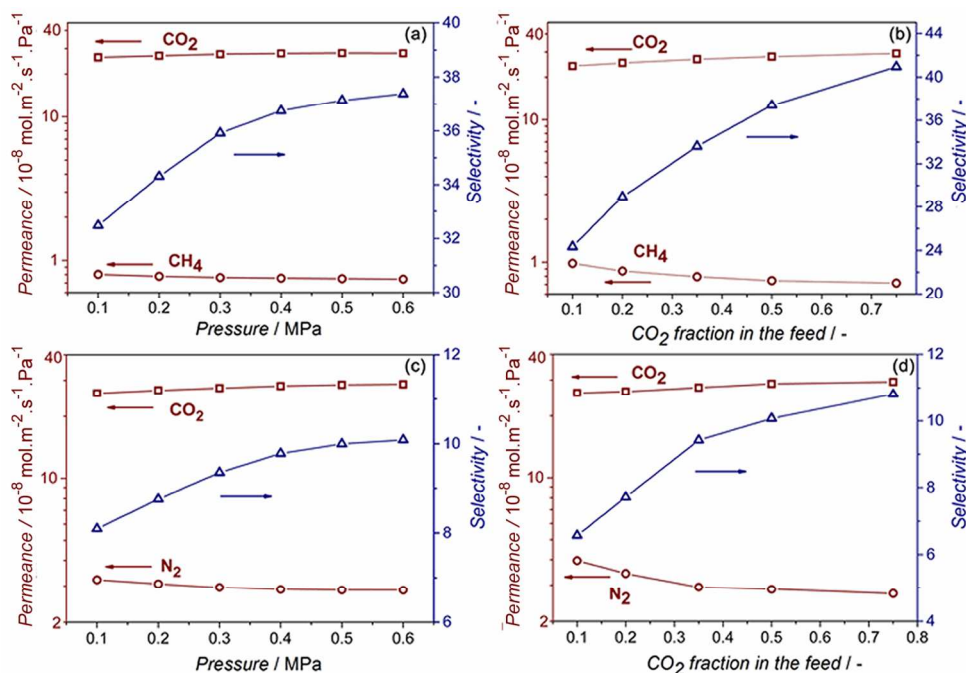


**Fig. 3** Separation of equimolar CO<sub>2</sub>/CH<sub>4</sub> (a) and CO<sub>2</sub>/N<sub>2</sub> (c) mixtures at varying pressure and influence of mixture composition on CO<sub>2</sub>/CH<sub>4</sub> (b) and CO<sub>2</sub>/N<sub>2</sub> (d) separation at a total pressure of 0.6 MPa (conditions: 293K, atmospheric pressure on permeate side, total flow rate 200 ml/min, 200 ml/min of sweep gas He).

This suggests that the separation is based on a combination of adsorption and diffusion selectivity. The common explanation for the higher selectivity of the mixture is that CO<sub>2</sub> molecules preferentially adsorb in the SSZ-13 pores and hinder the diffusion of the weaker adsorbing component.<sup>66</sup> Typically, the adsorption energy of CO<sub>2</sub> in zeolites increases with increasing polarity of the zeolite. Accordingly, saturation will occur at higher pressure for high-silica zeolites than for more polar low-silica zeolites.<sup>67</sup> Fig. 4 shows experimental adsorption isotherms of CO<sub>2</sub>, N<sub>2</sub> and CH<sub>4</sub> on SSZ-13 crystals together with simulated adsorption isotherms for the single components as well as for equimolar mixtures containing CO<sub>2</sub>. CO<sub>2</sub> adsorbs most strongly of all three adsorbates considered here (Fig. S9). The measured ideal adsorption selectivities at 0.1 MPa are ca. 12 and 5 for CO<sub>2</sub>/N<sub>2</sub> and CO<sub>2</sub>/CH<sub>4</sub>, respectively. The selectivities increase with decreasing pressure. This trend is consistent with the trend of the simulated single component adsorption isotherms. The simulation of adsorption isotherms of mixtures, however, shows that an increasing total pressure

results in an increased CO<sub>2</sub> selectivity. This peculiar phenomenon is not generally observed, but agrees with the results of Miyamoto *et al.*,<sup>38</sup> who experimentally studied CO<sub>2</sub> and N<sub>2</sub> mixture adsorption on pure-silica CHA. Increased adsorption selectivity explains the positive influence of total pressure and CO<sub>2</sub> partial pressure on the CO<sub>2</sub>/CH<sub>4</sub> and CO<sub>2</sub>/N<sub>2</sub> mixture separation selectivity by prepared SSZ-13 membranes (Fig. 3). This phenomenon is caused by disproportionately lower adsorption of the competing component when the pore occupancy of CO<sub>2</sub> increases with increasing CO<sub>2</sub> partial pressure. It derives from the stronger interaction of CO<sub>2</sub> with zeolites as well as from the stronger intermolecular interactions between CO<sub>2</sub> molecules than of CO<sub>2</sub> with N<sub>2</sub> or CH<sub>4</sub>, which may lead to cluster formation.<sup>68</sup> It is consistent with the modelling results showing that the presence of CH<sub>4</sub> or N<sub>2</sub> does not influence CO<sub>2</sub> adsorption, while CO<sub>2</sub> lowers CH<sub>4</sub> and N<sub>2</sub> adsorption substantially. Similar increase of selectivity has also been reported for CO<sub>2</sub>/H<sub>2</sub> separation by silicalite-1 (MFI) membranes.<sup>46</sup>

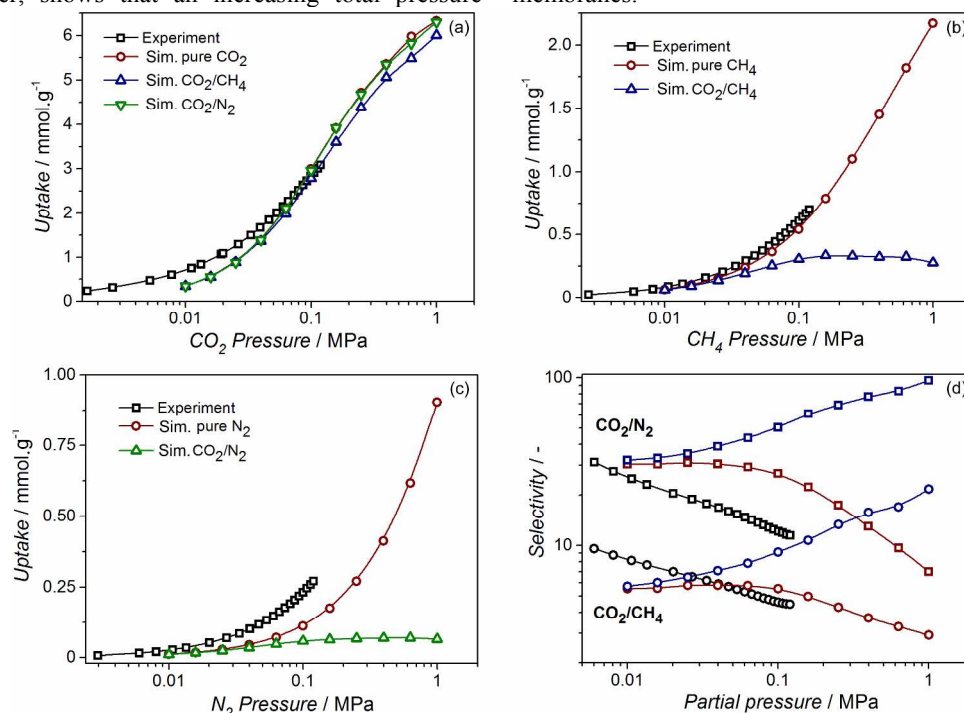


**Fig. 4** Experimental adsorption isotherms at 298 K and simulations of (a) CO<sub>2</sub>, (b) CH<sub>4</sub>, (c) N<sub>2</sub> on SSZ-13 powder (Si/Al = 80); (d) ideal and mixture adsorption CO<sub>2</sub>/CH<sub>4</sub> (circle) and CO<sub>2</sub>/N<sub>2</sub> (square) selectivities – experimental ideal (black), simulation single-gas (red), simulation mixture (blue).

#### Gas mixture separation: effect of temperature and humidity

The temperature dependence of CO<sub>2</sub>/CH<sub>4</sub> and CO<sub>2</sub>/N<sub>2</sub> separation performance was also studied (Fig. 5). As expected, an increase of the separation temperature leads to a decrease of the adsorption selectivity. At 473 K the values of the mixture separation become similar to those obtained in the single gas measurements. This finding implies that above 473 K the membrane operates in the Henry adsorption regime where the contribution of the peculiar adsorption selectivity at higher loadings becomes negligible and separation is governed by the diffusion selectivity times the ideal adsorption selectivity.<sup>69</sup>

Although water is typically present in most industrial gas streams, its influence on zeolite membrane performance is usually not investigated. Here, we compared gas mixture separation in dry and humid conditions to determine the

potential of the SSZ-13 membranes for separation of CO<sub>2</sub> from wet gas mixtures. For this purpose, the feed gas mixture was humidified by adding 2.2 kPa of water. Fig. 5 shows the results for the separation of dry and humidified CO<sub>2</sub>/CH<sub>4</sub>, and CO<sub>2</sub>/N<sub>2</sub> mixtures as a function of the temperature.

**Table 4** Permeance of gases at dry and humid conditions in separation of corresponding mixtures

Gas	Permeance / 10 <sup>-7</sup> mol.m <sup>-2</sup> .s <sup>-1</sup> .Pa <sup>-1</sup>					
	293 K, dry	293 K, Wet	% of dry	393 K, dry	393 K, wet	% of dry
CO <sub>2</sub> (N <sub>2</sub> )	2.8	0.71	25	1.9	1.6	84
N <sub>2</sub> (CO <sub>2</sub> )	0.27	0.04	15	0.36	0.31	86
CH <sub>4</sub> (CO <sub>2</sub> )	0.076	0.016	21	0.11	0.098	89

The presence of water affects the permeance of all the gases, which should be predominantly due to partial blockage of the zeolite pores. At 293 K the gas permeance is substantially lower under humid conditions compared to dry

conditions (Table 4). Due to the decreasing water coverage with increasing separation temperature, the permeance of all of the gases increases. Already at 393 K, the permeance under humid conditions is close to the permeance under dry conditions.

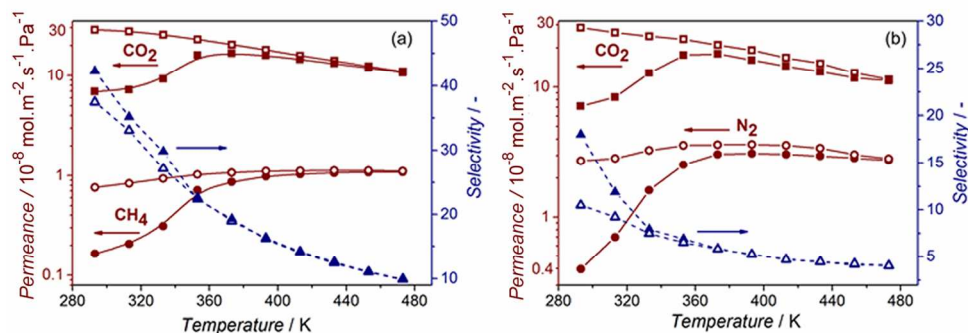


**Fig. 5** Separation of equimolar mixtures of (a) CO<sub>2</sub>/CH<sub>4</sub> and (b) CO<sub>2</sub>/N<sub>2</sub> (open symbols correspond to dry conditions, closed symbols to humid conditions, i.e. in the presence of 2.2 kPa of water; conditions: 0.6 MPa feed pressure, atmospheric pressure on permeate side, total flow rate 200 ml/min, 200 ml/min of sweep gas He).

In order to better understand the influence of humidity we also studied adsorption of water on SSZ-13 crystals. The results of such adsorption measurements are shown in Fig. 6.

hypothesis we studied the influence of humidity on SF<sub>6</sub> permeation. The results are collected in Fig. 7. In dry conditions SF<sub>6</sub> permeance gradually decreases with increasing temperature, which is characteristic for Knudsen (pore size 10–100 nm) and Poiseuille (pore size > 50 nm) flows.<sup>72</sup> The presence of water reduces the SF<sub>6</sub> permeance by ca. 50% at low temperature.

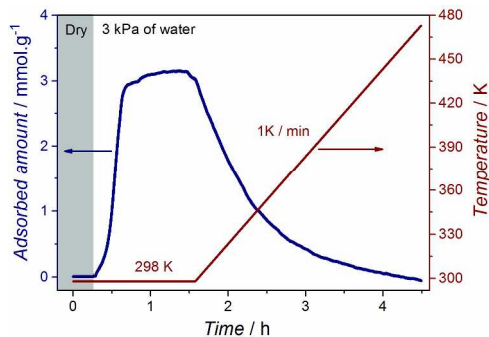


**Fig. 6** Adsorption of water on SSZ-13 (Si/Al = 100) crystals measured by TGA. During the experiment the sample was first completely dehydrated in dry He at 673 K, cooled down to 298 K and then subjected to a humidified (3 kPa H<sub>2</sub>O) He flow. After saturation the temperature was gradually increased to 473 K in the presence of the humidified He flow.

The amount of adsorbed water decreases from 3.1 mmol/g at 298 K to 0.32 mmol/g at 393 K. At 473 K the adsorbed amount of water was below the detection limit (~0.02 mmol/g). These results support our surmise that water partially blocks permeation of gases by adsorption into zeolite pores at low temperature. The hydrophobicity of high-silica SSZ-13 (Fig. S9) ensures nearly complete elimination of water adsorption at modest temperatures ~ 473K.<sup>70</sup>

A second important aspect of humidity is its influence on selectivity. CO<sub>2</sub>/N<sub>2</sub> and CO<sub>2</sub>/CH<sub>4</sub> mixture selectivities in the presence of water are higher than under dry conditions. The wet and dry selectivity values become similar in the 360–400 K temperature range. From the single-gas permeation data of a bulky SF<sub>6</sub> molecule and assuming this represents Knudsen diffusion through defects only, we can estimate the contribution of permeance through defects for other components (Fig. S10).<sup>71</sup> Expectedly, at 293 K there are larger contributions of permeance through defects for N<sub>2</sub> (~2%) and, especially, CH<sub>4</sub> (~9%) compared to CO<sub>2</sub> (~0.3%). Thus, partial blockage of non-zeolitic defects well explains the observed increase of selectivity under humid conditions. To further prove this

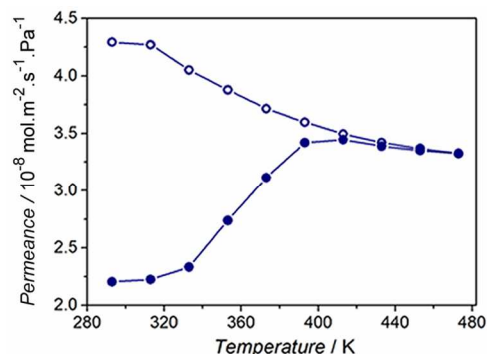


**Fig. 7** Influence of water on SF<sub>6</sub> single gas permeance (open symbols – dry gas, closed symbols – 2.2 kPa of water; conditions: 0.6 MPa feed pressure, atmospheric pressure on permeate side, total flow rate 200 ml/min, 200 ml/min of sweep gas He).

The difference with the dry permeation data decreases with increasing temperatures and becomes negligible above 410 K. We therefore conclude that water will adsorb on and block some of non-zeolitic pores at low temperature and, accordingly, improve the overall selectivity. It is also consistent with the proposed hydrophilic nature of such defects containing many silanols groups.<sup>73</sup>

### Membrane stability

Besides high permeance and selectivity, hydrothermal stability is one of the key advantages of zeolite membranes for application in technological settings.<sup>74,75</sup> We performed a CO<sub>2</sub>/N<sub>2</sub>/H<sub>2</sub>O (10/10/1) separation test at 393 K for 220 h. The results of this endurance test are shown in Fig. 8 and demonstrate that the membrane is stable under these conditions over the course of nearly 10 days. Despite a very small gradual increase of CO<sub>2</sub> and N<sub>2</sub> permeance, the selectivity did not

change. Hence, we argue that the slowly increasing permeance is not the result of deterioration of the zeolite structure but originates from, for instance, gradual degradation of amorphous material blocking some zeolite pores or other similar effects. Although the 220 h endurance test did not result in any deterioration of the membrane quality, more extended studies are necessary to verify the long-term stability of SSZ-13 membranes under industrially relevant conditions.

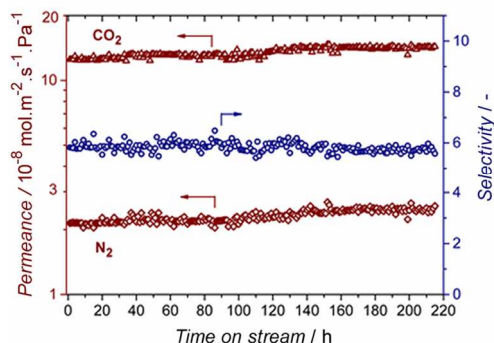


**Fig. 8** Membrane CO<sub>2</sub>/N<sub>2</sub>/H<sub>2</sub>O separation test (conditions: equimolar CO<sub>2</sub>/N<sub>2</sub> mixture, 393 K, 0.2 MPa feed pressure, 9.5 kPa of water, atmospheric pressure at permeate side, total flow rate 200 ml/min, 200 ml/min of sweep gas He).

Nevertheless, combined with the permeance and selectivity results, stability findings support our conclusion that high-silica SSZ-13 membranes are very promising candidates for separation of CO<sub>2</sub> from hot and humid gas streams (e.g. flue gases, product stream from methane steam reforming<sup>76</sup>) and from natural gas or biogas mixtures.

## Conclusions

High-silica SSZ-13 membranes were reproducibly prepared by hydrothermal secondary growth on the seeded inner surface of  $\alpha$ -alumina hollow fiber supports. At an Si/Al ratio of 86 they contain a low density of defects as characterized by the high H<sub>2</sub>/SF<sub>6</sub> ideal selectivity. Excellent performance was achieved in CO<sub>2</sub>/CH<sub>4</sub> and CO<sub>2</sub>/N<sub>2</sub> separation. The separation selectivity and CO<sub>2</sub> permeance increased with increasing total and CO<sub>2</sub> partial pressure, which is due to the preferred adsorption of CO<sub>2</sub> over the other competing component. The presence of water in the feed led to partial blockage of the zeolite pores as well as the more hydrophilic defects. Overall, it decreased permeance slightly, but increased the CO<sub>2</sub>/CH<sub>4</sub> and CO<sub>2</sub>/N<sub>2</sub> selectivity. These effects were most pronounced at temperatures below 400 K. The hydrophobic SSZ-13 membranes retained their beneficial separation properties during a long-term CO<sub>2</sub>/N<sub>2</sub> separation test under hydrothermal conditions. To summarize, the low polarity of the high-silica SSZ-13 membranes renders them promising candidates for separation of different CO<sub>2</sub>-containing mixtures at elevated pressure and temperature and in the presence of water vapor. The separation mechanism is based on a combination of adsorption and diffusion selectivity.

## Acknowledgements

Financial support from the STW-Hyflux Partnership Programme is gratefully acknowledged.

## Notes and references

<sup>a</sup> Schuit Institute of Catalysis, Laboratory of Inorganic Materials Chemistry, Eindhoven University of Technology, PO Box 513, 5600 MB Eindhoven, The Netherlands. E-mail: e.j.m.hensen@tue.nl, tel: +31-40-2475178

<sup>b</sup> Catalysis Engineering, ChemE, Delft University of Technology, Julianalaan 136, 2628 BL Delft, The Netherlands.

<sup>c</sup> Institute for Solid State Theory, University of Münster, Wilhelm-Klemm Str. 10, 48149 Münster, Germany.

† Electronic Supplementary Information (ESI) available: including schemes of experimental setup and membrane module, SEM images of support surface and seed layer, details of adsorption simulations, TGA analysis of detemplantation process, mixture separation in pressure gradient mode, water and gas adsorption isotherms, analysis of defect influence. See DOI: 10.1039/b000000x/

- [1] R.K. Pachauri, A. Reisinger, Eds. Fourth Assessment Report on Climate Change, International Panel on Climate change: Geneva, Switzerland, 2007.
- [2] M.Z. Jakobson, *Energy Environ. Sci.*, 2009, **2**, 148.
- [3] E.J. Stone, J.A. Lowe, K.P. Shine, *Energy Environ. Sci.*, 2009, **2**, 81.
- [4] Z.Z. Yang, L.N. He, J. Gao, A.H. Liu, B. Yu, *Energy Environ. Sci.*, 2012, **5**, 6602.
- [5] Zero Emission Platform (ZEP) report, The Costs of CO<sub>2</sub> Capture, Transport and Storage, 2011.
- [6] A. Maiti, *Quant. Chem.*, 2014, **114**, 163.
- [7] A.D. Ebner, J.A. Ritter, *Sep. Purif. Technol.*, 2009, **44**, 1273.
- [8] R.W. Baker, *Ind. Eng. Chem. Res.*, 2002, **41**, 1393.
- [9] E. Favre, *J. Membr. Sci.*, 2007, **249**, 50.
- [10] M. Pera-Titus, *Chem. Rev.*, 2014, **114**, 1413.
- [11] N. Du, H.B. Park, M.M. Dal-Cin, M.D. Guiver, *Energy Environ. Sci.*, 2012, **5**, 7306.
- [12] M. Anderson, H. Wang, Y.S. Lin, *Rev. Chem. Eng.*, 2012, **28**, 101.
- [13] Z. Zhang, Z.-Z. Yao, S. Xiang, B. Chen, *Energy Environ. Sci.*, 2014, DOI: 10.1039/C4EE00143E.
- [14] L. Diestel, X.L. Liu, Y.S. Li, W.S. Yang, J. Caro, *Microporous Mesoporous Mater.*, 2014, **189**, 210.
- [15] T. Rodenas, M. van Dalen, E. Garcia-Pérez, P. Serra-Crespo, B. Zornoza, F. Kapteijn, J. Gascon, *J. Adv. Funct. Mater.*, 2014, **24**, 249.
- [16] J. Caro, M. Noack, P. Kolsch, R. Schafer, *Microporous Mesoporous Mater.*, 2000, **38**, 3.
- [17] J. Gascon, F. Kapteijn, B. Zornoza, V. Sebastian, C. Casado, J. Coronas, *Chem. Mater.*, 2012, **24**, 2829.
- [18] Z. Lai, G. Bonilla, I. Diaz, J.G. Nery, K. Sujaoti, M.A. Amat, E. Kokkoli, O. Terasaki, R.W. Thompson, M. Tsapatsis, D.G. Vlachos, *Science*, 2003, **300**, 456.
- [19] J.M. v.d. Graaf, F. Kapteijn, J.A. Moilijn, *Chem. Eng. Sci.*, 1999, **54**, 1081.
- [20] J.A. Stoeger, J. Choi, M. Tsapatsis, *Energy Environ. Sci.*, 2011, **4**, 3479.
- [21] J. Hedlund, J. Sterte, M. Anthonis, A.-J. Bons, B. Carstensen, N. Corcoran, D. Cox, H. Deckman, W. De Gijnst, P.-P. de Moor, F.

- Lai, J. McHenry, W. Mortier, J. Reinoso, J. Peters, *Microporous Mesoporous Mater.*, 2002, **52**, 179.
- [22] T.C. Pham, H.S. Kim, K.B. Yoon, *Science*, 2011, **334**, 1533.
- [23] L. J. P. van den Broeke, W. J. W. Bakker, F. Kapteijn, J. A. Moulijn, *AIChE J.*, 1999, **45**, 976.
- [24] X. Zhu, H. Wang, Y.S. Lin, *Ind. Eng. Chem. Res.*, 2010, **49**, 10026.
- [25] Z. Lixiong, J. Dong, M. Enze, *Stud. Surf. Sci. Catal.*, 1997, **105**, 2211.
- [26] J.C. Poshusha, V.A. Tuan, J.L. Falconer, R.D. Noble, *Ind. Eng. Chem. Res.*, 1998, **37**, 3924.
- [27] S. Li, J.L. Falconer, R.D. Noble, *J. Membr. Sci.*, 2004, **241**, 121.
- [28] W. Lutz, R. Kurzhals, S. Sauerbeck, H. Toufar, J.-Chr. Buhl, T. Gesing, W. Altenburg, Chr. Jäger, *Microporous Mesoporous Mater.*, 2010, **132**, 31.
- [29] J.C. Poshusta, R.D. Noble, J.L. Falconer, *J. Membr. Sci.*, 2001, **186**, 25.
- [30] J. Caro, M. Noack, *Microporous Mesoporous Mater.*, 2008, **115**, 215.
- [31] M. Noack, P. Kolsch, V. Seefeld, P. Toussaint, G. Georgi, J. Caro, *Microporous Mesoporous Mater.*, 2005, **79**, 329.
- [32] T. Tomita, K. Nakayama, H. Sakai, *Microporous Mesoporous Mater.*, 2004, **68**, 71.
- [33] J. Kuhn, K. Yajima, T. Tomita, J. Gross, F. Kapteijn, *J. Membr. Sci.*, 2008, **321**, 344.
- [34] L. Wu, V. Degirmenci, P.C.M.M. Magusin, N.J.H.G.M. Lousberg, E.J.M. Hensen, *J. Catal.*, 2013, **298**, 27-40.
- [35] M.R. Hudson, W.L. Queen, J.A. Mason, D.W. Fickel, R.F. Lobo, C.M. Brown, *J. Am. Chem. Soc.*, 2012, **134**, 1970.
- [36] T.D. Pham, Q. Liu, R.F. Lobo, *Langmuir*, 2012, **29**, 832.
- [37] M. Miyamoto, Y. Fujioka, K. Yogo, *J. Mater. Chem.*, 2012, **22**, 20186.
- [38] X. Li, H. Kita, Z. Zhang, K. Tanaka, K.-I. Okamoto, *Microporous Mesoporous Mater.*, 2011, **143**, 270.
- [39] K. Sato, K. Sugimoto, N. Shimotsuma, T. Kikuchi, T. Kyotani, T. Kurata, *J. Membr. Sci.*, 2012, **409-410**, 82.
- [40] H. Kalipcilar, T.C. Bowen, R.D. Noble, J.L. Falconer, *Chem. Mater.*, 2002, **14**, 3458.
- [41] N. Yamanaki, M. Itakura, Y. Kiyozumi, Y. Ide, M. Sadakane, T. Sano, *Microporous Mesoporous Mater.*, 2012, **158**, 141-147.
- [42] A. Huang, J. Caro, *J. Membr. Sci.*, 2012, **389**, 272.
- [43] K. Kusakabe, T. Kuroda, K. Uchino, Y. Hasegawa, S. Morooka, *AIChE J.*, 2004, **45**, 1220.
- [44] K. Weh, M. Noack, I. Sieber, J. Caro, *Microporous Mesoporous Mater.*, 2002, **54**, 27.
- [45] M. Zhou, D. Korelskiy, P. Ye, M. Grahn, J. Hedlund, *Angew. Chem. Int. Ed.*, 2014, **53**, 3492..
- [46] L. Sandstrom, E. Sjöberg, J. Hedlund, *J. Membr. Sci.*, 2011, **380**, 232.
- [47] A. Huang, N. Wang, J. Caro, *Microporous Mesoporous Mater.*, 2012, **164**, 294.
- [48] S. Li, J.G. Martinek, J.L. Falconer, R.D. Noble, *Ind. Eng. Chem. Res.*, 2005, **44**, 3220.
- [49] R. Zhou, E.W. Ping, H.H. Funke, J.L. Falconer, R.D. Noble, *J. Membr. Sci.*, 2013, **444**, 384.
- [50] Y. Tian, L. Fan, Z. Wang, S. Qui, G. Zhu, *J. Mater. Chem.*, 2009, **19**, 7698.
- [51] S. Himeno, T. Tomita, K. Suzuki, K. Nakayama, K. Yajima, S. Yoshida, *Ind. Eng. Chem. Res.*, 2007, **46**, 6989.
- [52] J. van der Bergh, W. Zhu, J. Gascon, J.A. Moulijn, F. Kapteijn, *J. Membr. Sci.*, 2008, **316**, 35.
- [53] Y. Cui, H. Kita, K.-I. Okamoto, *J. Mater. Chem.*, 2004, **14**, 924.
- [54] A. Chrakhi, H. Kazemian, M. Kazemini, *Powder Technol.*, 2010, **209**, 389.
- [55] E. García-Pérez, J.B. Parra, C.O. Ania, A. García-Sánchez, J.M. van Baten, R. Krishna, D. Dubbeldam, S. Calero, *Adsorption*, 2007, **13**, 469.
- [56] N. Kosinov, E.J.M. Hensen, *J. Membr. Sci.*, 2013, **447**, 12.
- [57] N. Kosinov, G. Sripathi, E.J.M. Hensen, 2014, *Microporous Mesoporous Mater.*, 2014, **194**, 24.
- [58] A. Navajas, R. Mallada, C. Tellez, J. Coronas, M. Menendez, J. Santamaria, *J. Membr. Sci.*, 2007, **299**, 166.
- [59] I.G. Giannakopoulos, V. Nikolakis, *Ind. Eng. Chem. Res.*, 2005, **44**, 226.
- [60] H.H. Funke, M.Z. Chen, A.N. Prakash, J.L. Falconer, R.D. Noble, *J. Membr. Sci.*, 2014, **456**, 185.
- [61] E.A. Eilertsen, B. Arstad, S. Svelle, K.P. Lillerud, *Microporous Mesoporous Mater.*, 2012, **153**, 94.
- [62] M. A. Carreon, S. Li, J.L. Falconer, R.D. Noble, *J. Am. Chem. Soc.*, 2008, **130**, 5412.
- [63] J. van der Bergh, A. Tihaya, F. Kapteijn, *Microporous Mesoporous Mater.*, 2010, **132**, 137.
- [64] F. Kapteijn, J. M. van de Graaf, J. A. Moulijn, *AIChE J.*, 2000, **46**, 1096.
- [65] J. van der Bergh, W. Zhu, J. Gascon, J. A. Moulijn, F. Kapteijn, *J. Membr. Sci.*, 2008, **316**, 35.
- [66] F. Kapteijn, J. M. van de Graaf, J. A. Moulijn, *J. Molec. Catal. A: Chem.*, 1998, **134**, 201.
- [67] M. Palomino, A. Corma, F. Rey, S. Valencia, *Langmuir*, 2010, **26**, 1910.
- [68] V.D. Borman, V.V. Teplyakov, V.N. Tronin, I.V. Tronin, V.I. Troyan, *J. Exp. Theor. Phys.*, 2000, **90**, 950.
- [69] J.M. van der Graaf, F. Kapteijn, J.A. Moulijn, *AIChE J.*, 1999, **45**, 497.
- [70] B. Hunger, S. Matysik, M. Heuchel, E. Geidel, H. Toufar, *J. Therm. Anal.*, 1997, **49**, 553.
- [71] J. van der Bergh, C. Gücüyener, J. Gascon, F. Kapteijn, *Chem. Eng. J.*, 2011, **166**, 368.
- [72] F. Jareman, J. Hedlund, D. Creaser, J. Sterte, *J. Membr. Sci.*, 2004, **236**, 81.
- [73] M. Noack, P. Kolsch, A. Dittmar, M. Stohr, G. Georgi, M. Schneider, U. Dingerdissen, A. Feldhorf, J. Caro, *Microporous Mesoporous Mater.*, 2007, **102**, 1.
- [74] Poshusta, J. C.; Noble, R. D.; Falconer, J. L. *J. Membr. Sci.*, 2001, **186**, 25.

- [75] S. Himeno, T. Tomita, K. Suzuki, S. Yoshida, *Microporous Mesoporous Mater.*, 2007, **98**, 62.
- [76] M. E. Ayturk, N.K. Kazantzi, Y. H. Ma, *Energy Environ. Sci.*, 2009, **2**, 430.